**Proceedings of ASME Turbo Expo 2011**
**GT2011**
**June 6-10, 2011, Vancouver, British Columbia, Canada**

**GT2011-45489**

# PROCESS INTEGRATION AND AUTOMATED NUMERICAL DESIGN OPTIMIZATION OF AN EIGENFREQUENCY ANALYSIS OF A COMPRESSOR BLADE

**Philipp Hecker, Damir Delimar, Herbert Brandl, Michael Lötzerich**
Alstom Power
Baden, Switzerland

## ABSTRACT

Modern gas turbines for applications in power plants have to fulfill more and more demands defined by customer and grid requirements. These requirements address for example reduced time for run up and increased power output while providing maximum single or combined cycle efficiency. The demanding market requirements increase the pressure to further improve the design process of gas turbine parts by reducing the overall development time and simultaneously improving the quality of the design.

This paper describes the implementation of an automated optimization process for the mechanical assessment of compressor blades applied during the preliminary design process. Previous work from Fedorov, Szwedowicz, et al [1], has shown that it is important to apply 3D FE methods for the accurate prediction of the dynamic behavior of compressor blades already in the early stage of the design phase. These key ideas were picked up in the present work while the FE model from [1] was extended to a complete 3D model of the compressor blade including airfoil and blade root geometry.

The new approach completely automates the 3D FE analysis of compressor blades including CAD model generation, FE pre-processing, FE analyses, FE post-processing and takes it to the further level by integrating the FE analysis procedure into an automated design loop using the commercial optimization software iSight FD. The target of this optimization loop is to drive the frequency of critical mode shapes into allowed ranges by modifying airfoil parameters such as airfoil thickness and chord length. A scalar optimization technique is applied solving the design problem using penalty functions for excitation sources, mode shapes and eigenfrequencies. In order to achieve a smooth distribution of airfoil parameters Bezier-Spline approximations are used to parameterize the design space.

The implementation of the mechanical analysis for compressor blades into a standardized and automated process was one of the main achievements of the presented work. The process was completely implemented in Abaqus CAE including 3D FE model preparation and post-processing. It was key to a successful integration into an overall optimization loop, which helped to substantially reduce the amount of manual work required to perform the design task.

## NOMENCLATURE

| | |
|---|---|
| FE | Finite Element |
| $f_{EO}$ | Excitation frequency |
| $\Delta f_{EO}$ | Prohibited frequency range |
| $N$ | Number of vanes |
| $n$ | Rotational speed |
| $f_M$ | Eigenfrequency of a specific eigenmode |
| $p$ | Penalty value |

| | |
|---|---|
| *t(s)* | Profile thickness depending on airfoil section |
| *c(s)* | Chord length depending on airfoil section |
| *CP* | Control point |
| *s* | Airfoil section |
| *CFR* | Compound fillet radius |
| *CFR1* | Compound fillet radius 2 |
| *CFH* | Compound fillet height |
| $\eta$ | Speed weighting factor |
| $d_1, d_2$ | Frequency range factor |

Subscripts

| | |
|---|---|
| *nom* | Nominal |
| *i* | Speed index |
| *j* | Excitation index |
| *k* | Eigenmode index |
| *min* | Minimum value |
| *max* | Maximum value |
| *EO* | Engine order |
| *M* | Mode |
| *F* | Frequency |
| *sum* | Sum |
| *ll* | Lower limit |
| *ul* | Upper limit |
| *a,b* | Control point index |
| *L* | Loose fixation |
| *T* | Tight fixation |

## BACKGROUND APPLICATION OF NUMERICAL OPTIMIZATION METHODS

In response to the increasing market demands Alstom is continuously improving its design processes used for component design and gas turbine integration. The work from Fedorov, Szwedowicz, et al [1], enabled Alstom to predict more accurately the eigenfrequencies of compressor blades. They showed that simple beam-model based methods are fast and accurate enough for predicting airfoil stresses and eigenfrequencies of lower order modes. Higher order modes, however, cannot be predicted by applying a 1D approach within acceptable accuracy why they first introduced a 3D FE based process for the prediction of higher order modes such as chord-wise bending. Further, different blade restraints have been considered in order to reduce uncertainties due to different blade fixations.

Further projects performed at Alstom [2] concentrated on shrouded turbine blades. Here, 1D, 2D and 3D analyses have been combined in a design process assessing effects of airfoil stresses and untwisting effects during operation. Furthermore, a multi-objective optimization has been implemented in order to define optimal parameter values defining the initial blade shroud clearance and coupling angle.

In general concerning design processes of complex engineering products like gas turbines the early design phase is quite important as it enables the engineer to explore as many designs as possible, [3]. A further paper [4] shows how important the understanding of different cost drivers of a gas turbine component becomes in case manufacturing costs of a preferred design have to be judged against operating costs. This task is typically defined as an optimization problem judged in the early design phase. Hence, the preliminary design phase is one of the most common instances of applying numerical optimization methods. Consequently, [5] introduces a preliminary, multi-disciplinary optimization process for the aerodynamic assessment of a compressor design. In this work the calculation of flow parameters along compressor meanline is linked with the mechanical assessment of compressor discs using a 1D approach. Later an approach replacing the 1D model by 3D methods for the more accurate prediction of the mechanical behavior of the complete bladed disc is introduced.

As the detailed design phase progresses 1D models are gradually replaced by more accurate 3D methods in order to further reduce the uncertainty in the design. For example [6] describes 3D CFD optimization of a compressor blade applying an artificial neuronal network in combination with a genetic optimization algorithm. A similar approach has been chosen by [7] optimizing the aerodynamic performance of a compressor blade by modifying sweep and lean of the airfoil. Introducing more design criteria leads to a multi-objective optimization applied to a tandem compressor cascade [8] where pressure ratio and blade losses are optimized by modifying blade camber line and thickness distribution. In this work an artificial neuronal network was successfully applied in combination with a multi-objective genetic algorithm (MOGA) in order to reduce the computation effort.

In addition to aerodynamic aspects major effort is also invested in the mechanical analysis of gas turbine parts, [9] gives examples of applying numerical optimization methods for the optimization of a turbine blade – disc attachment with the objective to maximize the turbine disc life and determining effects of manufacturing tolerances on a compressor disc. Further work [10] investigated effects of parameter variations on a secondary air system as well as on the thermal mechanical behavior of a turbine system.

The work published in [11] and [12] assesses the optimization of aero engine fan stages, where [11] realizes a combined aerodynamic and mechanical approach for the multi-disciplinary optimization of a counter-rotating fan. Here, the preliminary-axisymmetric design is complemented by a three-dimensional multi-stage analysis. The 3D optimization loop includes aerodynamic parameters like peak efficiency and pressure ratio as well as mechanical criteria like stresses and allowable eigenfrequency ranges. The application of surrogate models using radial basis functions helped to reduce the required computing effort.

## AUTOMATED MECHANICAL ASSESSMENT OF COMPRESSOR BLADES

Figure 1 shows a sketch of a 22-stage GT26 compressor cross-section. Due to the large amount of blade rows a family design was chosen for the blade root fixation in order to keep the design effort and costs low. With the exception of some vanes and blades a common hammer foot style was developed for the blade root fixation. Figure 2 shows a sketch of a compressor blade and vane with a standard hammer foot fixation. With respect to the optimization task the standardized blade fixation proved to be useful since it allowed the use of a common parametric model for almost all of the blade rows.

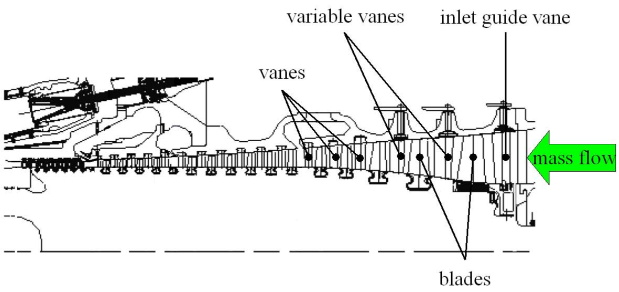


**Figure 1: 22-stage gas turbine compressor GT26**

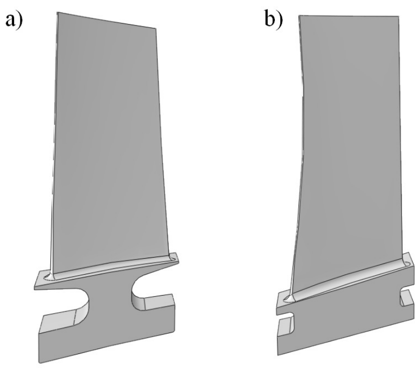


**Figure 2: Compressor blade a) and vane b) with hammer foot fixation**

During the preliminary design phase several iterative loops between aerodynamic and mechanical disciplines are performed, Figure 3. Once the aerodynamic design of a blade is completed performing a series of automated 3D FE analyses assesses the mechanical behavior. In case the lifetime requirements are not fulfilled the blade geometry is modified or in case the airfoil needs to be changed the loop is repeated.

The mechanical analysis has been automated and fully implemented in Abaqus CAE. The model building steps include parametric CAD model generation, meshing, and solver input preparation. Subsequent to the FE analyses, a post-processing routine is called which collects all relevant information on stresses in the critical airfoil and blade root regions. Information on blade eigenfrequencies for different blade fixations and load cases is also extracted. The main scope of this work is on the automated mechanical analysis, the aerodynamic design step shown in Figure 3 is not incorporated.

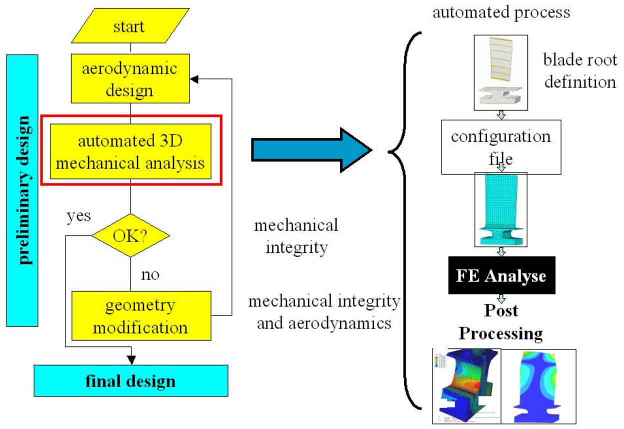


**Figure 3: Design process compressor blade**

Input to the 3D CAD model generation process step is a point wise description of the airfoil based on streamline sections complemented by a set of parameters describing the parametric blade root geometry. The airfoil solid is based on an underlying wire construction of 21 streamline sections or profile sections. The blade root solid is described by a set of 15 parameters. The final CAD model is build by fusing the airfoil solid with the blade root solid and applying a compound fillet transition between the two solids. The compound fillet is modeled by means of three parameters, two different fillet radii and a parameter describing the compound fillet height.

With respect to the FE loads a uniform temperature, a centrifugal load depending on the engine speed and a pressure field acting on the complete airfoil region are applied. According to Alstom experience, [1], two blade fixations are considered: loose and tight, Figure 4a, b. The idea behind the loose fixation is that only the blade-rotor-contact faces are taking the load while in case of tight fixation additional contact surfaces between the neighboring blades are clamped. The surfaces which are used to define the restraints for the loose and tight fixation are highlighted in Figure 4 while the node elements are fixed in all directions at these locations. In the real engine the blade eigenfrequencies are expected to range within the calculated limits of loose and tight fixation. The calculated eigenfrequencies for the different blade fixations may vary in a range of up to ten percent depending on the root geometry. In summary six FE analyses are performed within preliminary design to ensure all lifetime requirements are met:

- 1 static analysis
- 4 modal analyses for different load cases and fixations
- 1 limit load analysis.

The FE mesh used in this work typically consists of around 35000 nodes while quadratic wedge elements are applied for the airfoil partition and tet elements in the lower part of the blade. Information on mesh size and element types can be found in Table 1. A first mesh sensitivity study revealed no indication of a mesh dependency on the calculated eigenfrequencies. A more detailed mesh sensitivity analysis is planned in the future with the objective to explore the potential of further reducing the computational time.

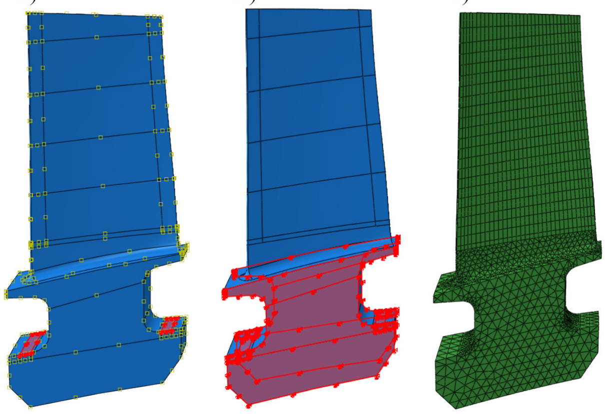


**Figure 4: Visualization of boundary conditions, loose (a), tight (b) and applied FE mesh (c)**

**Table 1: Mesh properties of the considered blade geometry**

| | |
|---|---|
| Number of elements | 18600 |
| Number of Nodes | 35200 |
| FE type airfoil | Quadratic wedges, C3D15 |
| FE type root | Quadratic tets, C3D10 |

## DEFINITION OF THE OPTIMIZATION PROBLEM

The design problem discussed in this paper is primarily related to the dynamic behavior of a compressor blade regarding blade eigenfrequencies. Several eigenmodes and their corresponding frequencies are checked starting from simple modes, like first weak bending, and moving to more complex eigenmodes, like chord-wise bending, see Figure 5. In this paper an example of a first blade design out of a concept study is assessed. Therefore, an old airfoil design has been scaled and placed in a new engine environment. The resulting Campbell diagram of the considered compressor blade is shown in Figure 6, where eigenfrequencies and excitation frequencies are plotted against engine speed. The intersections between excitation engine orders and eigenfrequencies for a specific engine speed line indicates areas having a potential risk of blade resonances.

During normal engine operation when individual compressor blades may be exposed to rubbing, erosion or corrosion, eigenmodes running in resonance could also contribute to a significant degradation of the blade lifetime.

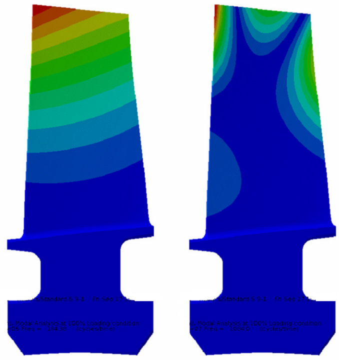

**Figure 5: Visualization of blade eigenmodes for first weak bending and first chord-wise bending**

The red box in Figure 6 shows an example of an excitation of several eigenfrequencies of the rotating blade caused by the passing wakes of an excitation source. The frequency of this excitation scales linearly with the number of vanes, struts or other excitation sources $N$ and the rotational speed $n$:

$$f_{EO} = N \cdot n \,. \qquad \textbf{Equation 1}$$

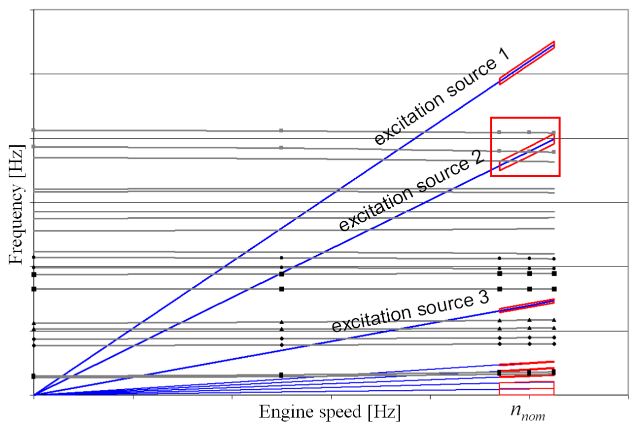


**Figure 6: Campbell diagram of a compressor blade**

In order to keep a safety distance between blade eigenfrequencies and excitations a prohibited frequency range is defined $\Delta f_{EO}$ defined by:

$$\Delta f_{EO} = (1 \pm d_1) \cdot N \cdot n \,, \qquad \textbf{Equation 2}$$

where $d_1$ is a parameter defined according to Alstom experience.

The growing number of design relevant modes has fostered the need for developing an automated frequency tuning assessment tool with the objective to use numerical optimization methods to find acceptable solutions. In order to allow an automated process to handle this task, the visual assessment of the Campbell diagram, Figure 6, was coded into a computer program. The strategy for the frequency check is based on the idea of introducing frequency penalties as applied in a similar way by [13], [11] and [12]. For each eigenmode pair of loose and tight blade fixation an upper and lower frequency limit can be determined. The resulting frequency range is not allowed to intersect the excitation lines.

For the implementation into the optimization process two terms are defined: a) a feasible design in case the mode pairs are located completely outside of the prohibited area and b) an infeasible design in case at least one mode pair intersects the prohibited area. Examples for feasible/infeasible designs are given in Figure 7, where the mode pairs of design examples 1 and 2 are outside of the prohibited frequency range. In order to come up with a robust design characterized by a reduced risk of violating the prohibited frequency range an additional safety factor is introduced to account for manufacturing variations and uncertainties in blade fixation. The circles around the points L, T (loose and tight eigenfrequency of a specific eigenmode) in Figure 7 reflect this additional safety factor. The frequency range is defined as

$$f_{M,\min} = (1 - d_2) \cdot f_M \qquad \textbf{Equation 3}$$

and

$$f_{M,\max} = (1 + d_2) \cdot f_M \qquad \textbf{Equation 4}$$

with $M \in [L, T]$.

The analyses of loose and tight eigenfrequencies revealed, that

$$f_T \approx (1 + 2d_2) \cdot f_L . \qquad \textbf{Equation 5}$$

Further the resulting frequency range defined by $f_{M,\min}$ and $f_{M,\max}$ covers all eigenfrequency variations due to manufacturing tolerances. The resulting frequency ranges for excitation and eigenmodes including the defined safety factors are shown in Figure 8.

In order to assess the eigenfrequencies of a given design, the following steps have been implemented into the frequency-tuning tool:

1. Move through all design relevant engine speeds, $i \in [n_{\min}, n_{\max}]$.
2. Move through all relevant excitation sources, $j \in [EO_{\min}, EO_{\max}]$.
3. Move through all relevant eigenmodes, $k \in [M_{\min}, M_{\max}]$.

Taking Figure 8 as an example, the following frequency criteria have to be fulfilled:

$$\Delta f_{EO,i,j+1,\min} \geq f_{M,i,k,\max}$$

and **Equation 6**

$$\Delta f_{EO,i,j,\max} \leq f_{M,i,k,\min} ,$$

with $M \in [L, T]$.

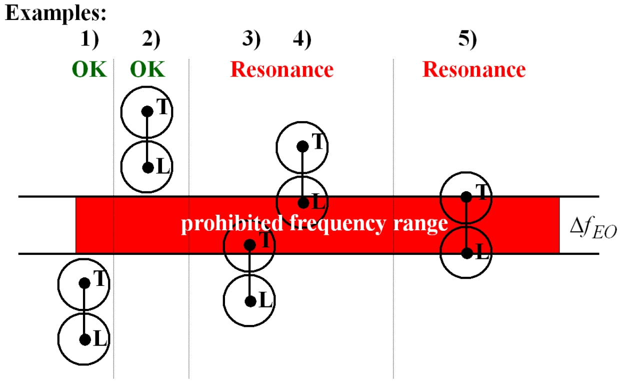


**Figure 7: Position of eigenfrequency mode pairs relative to the prohibited frequency range**

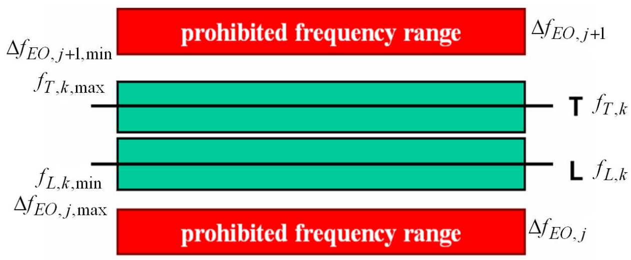


**Figure 8: Enhanced eigenfrequency area taking into account variation in manufacturing**

In case Equation 6 is violated, penalty terms are defined depending on the excitation source, the eigenmode in resonance and the size of overlapping between prohibited frequency range and eigenfrequency range. Examples of excitation penalty factors and mode penalty factors, which are used to weight the different excitation sources and modes, are given in Table 2 and Table 3. The shown values have arbitrarily been chosen with a proper weighting to each other. For the presented example, excitation 2 is assumed to represent the most sensitive excitation source concerning blade resonances and possible damages. Excitations caused by sources 1 and 3 are assumed to have less effect on blade lifetime, hence their lower penalty values.

**Table 2: Excitation penalty factor**

| Excitation source | Penalty factor $p_{EO}$ |
|---|---|
| Lower Engine orders | 100 |

| | |
|---|---|
| Excitation source 2 | 100 |
| Excitation source 1 | 50 |
| Excitation source 3 | 25 |
| Any other excitation | 10 |

**Table 3: Mode penalty factor**

| **Mode number** | **Penalty factor** $p_M$ |
|---|---|
| 1 | 150 |
| 2 | 140 |
| 3 | 130 |
| 4 | 120 |
| 5 | 110 |
| 6 | 100 |
| 7 | 100 |
| 8 | 100 |
| 9 | 100 |
| 10 | 100 |
| 11 | 100 |
| 12 | 50 |

The frequency penalty factor reflecting a possible frequency overlapping between eigenfrequency range and prohibited frequency range is defined as follows:

$$p_{F,i,j,k} = \min\left(f_{M,i,k,\max}, \Delta f_{EO,i,j,\max}\right) - \max\left(f_{M,i,k,\min}, \Delta f_{EO,i,j,\min}\right) \quad \textbf{Equation 7}$$

In the following, the three penalty terms for a specific speed $i$ are multiplied resulting in the penalty value

$$p_i = p_{EO,i,j} \cdot p_{M,i,j,k} \cdot p_{F,i,j,k}, \forall j,k . \quad \textbf{Equation 8}$$

The resulting penalty sum of a specific design is defined by summing the penalty results of all considered speeds:

$$p_{sum} = \sum_i \eta_i \cdot p_i , \quad \textbf{Equation 9}$$

where $\eta_i$ is a factor weighting the speeds. Finally, the optimization problem is reduced to the following function:

$$\min[p_{sum}] . \quad \textbf{Equation 10}$$

Further constraints need to be defined limiting airfoil stresses and requirements concerning aerodynamic properties of the airfoil.

## OPTIMIZATION PARAMETERS

Following design parameters are modified in the course of the optimization process, where $s$ denotes the radial position of a profile section:

- Profile thickness $t(s)$
- Chord length $c(s)$
- Compound fillet parameters $CFR, CFR1, CFH$ .

In order to ensure sufficient design freedom and to guarantee a smooth airfoil geometry, 3rd order Bezier-Splines (4 control points) are used for the approximation of the parameters, Figure 9 and Figure 10. The first control point of the Bezier-Spline (hub section) and the last control point (tip section) are not allowed to be moved in radial direction and are therefore fixed in s-direction.

In combination with the compound fillet parameters, the complete design problem can be described by 15 parameters limited by parameter constraints. The compound fillet is modified by:

$$CFR_{ll} \le CFR \le CFR_{ul} , \quad \textbf{Equation 11}$$

$$CFR1_{ll} \le CFR1 \le CFR1_{ul} , \quad \textbf{Equation 12}$$

$$CFH_{ll} \le CFH \le CFH_{ul} . \quad \textbf{Equation 13}$$

The control point parameters describing the approximation of thickness und chord length are varied according to:

$$CP_{a,x,ll} \le CP_{a,x} \le CP_{a,x,ul} , \quad \textbf{Equation 14}$$

for the number of control points $a \in [1,2,3,4]$ and

$$CP_{b,y,ll} \le CP_{b,y} \le CP_{b,y,ul} , \quad \textbf{Equation 15}$$

for $b \in [2,3]$.

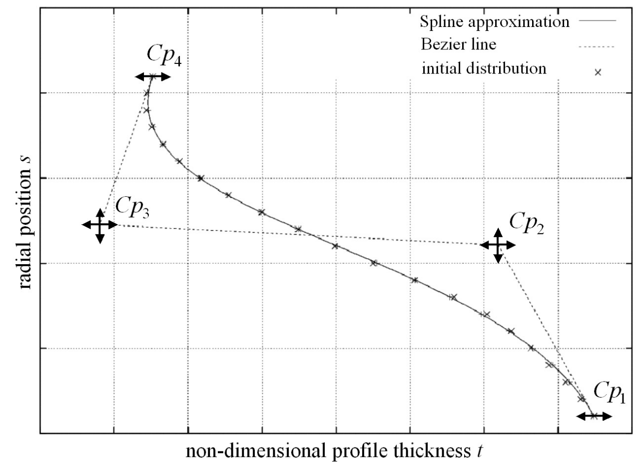


**Figure 9: Bezier-Spline approximation of profile thickness depending on radial position**

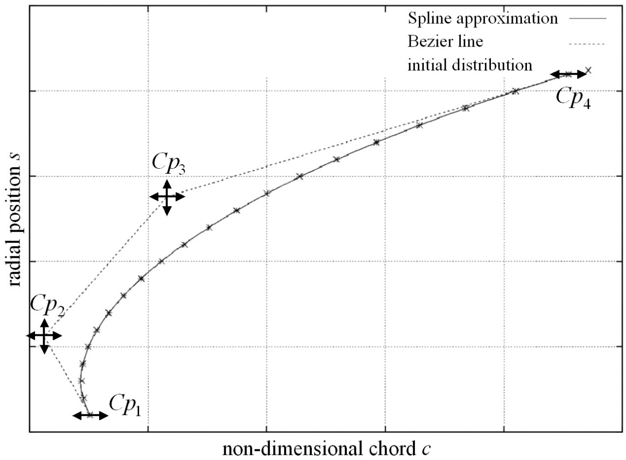


**Figure 10: Bezier-Spline approximation of chord length depending on radial position**

## CONSTRAINTS

During the optimization process predefined constraints have to be considered in addition to the penalty criterion. The first constraint defines a maximum worsening of the penalty value relative to a defined limit

$$p_{sum} \leq p_{sum,ul} \, . \qquad \textbf{Equation 16}$$

In case a solution exceeds the maximum allowable penalty sum it is marked as infeasible and is therefore not considered for future design iterations. This helps the optimization algorithm to converge faster.

A further constraint has been defined limiting the minimum allowable eigenfrequency of the compressor blade. This limit is defined according to Alstom experience

$$\min\left(f_{M,i,j,k}\right) \geq f_{ll,i} \qquad \textbf{Equation 17}$$

with

$$f_{ll,i} = 2 \cdot n_i \, . \qquad \textbf{Equation 18}$$

## OPTIMIZATION STRATEGY

The optimization strategy chosen for the frequency-tuning problem is based using the results of the 3D FE analysis for the assessment of each individual design. When using 3D FE analyses for optimization the computational time may become critical. The overall computational time for the present problem did not exceed 5 days mainly due to the usage of parallel CPU resources. The optimization problem has been solved by applying MIGA (multi-island genetic algorithm) as optimization algorithm.

## IMPLEMENTATION INTO ISIGHT

The automated frequency tuning process has been implemented in the commercial process integration und design optimization software iSight FD 3.5. The top-level process is split into two main components. The first sub-process, the initialization, provides an initial set of design data for thickness and chord distribution as well as a starting compound fillet design. The second sub-process performs the optimization loop, Figure 11.
During the optimization loop the following tasks are performed

- Define design parameters of the new compressor blade geometry, parameter modification
- Save modified geometry parameters into configuration files applied for geometry generation
- Automated 3D CAD model generation
- Automated 3D FE analysis
- Automated post-processing and design evaluation according to the defined penalty strategy

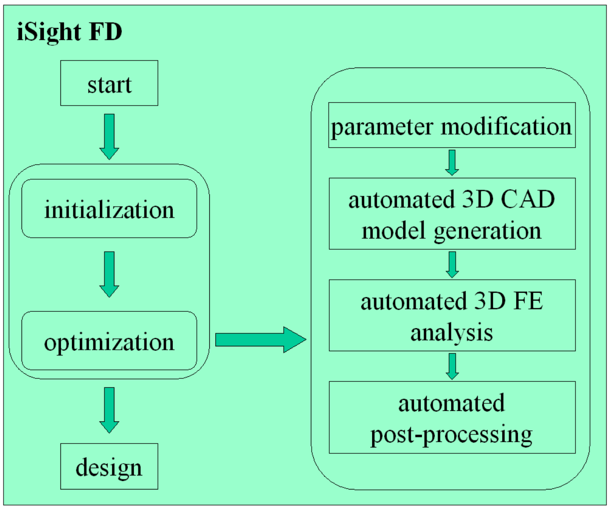


**Figure 11: Automated design loop implemented in iSight FD 3.5**

## RESULTS

In the following a short overview on the design solution of the assessed preliminary blade design is given which was obtained by using MIGA as optimization algorithm with the following settings:

- Sub population size: 10,
- Number of islands: 3,
- Number of generations: 20,
- Interval of migration: 5,
- Elite size: 1.

More information on setting up a genetic optimization algorithm can be found in [14]. After a runtime of approximately one hundred hours and approximately six hundred 3D FE design evaluations the optimization run stopped. The penalty values applied for this optimization have already been introduced in Table 2 and Table 3.

The convergence history of the optimization run is depicted in Figure 12 showing the evolution of the penalty sum $p_{sum}$ versus iteration number. The red line in Figure 12 reflects the constraint limiting the maximum allowable worsening of the design criterion. After approximately three hundred iterations already a design has been determined which is quite close to the final solution, **2** in Figure 12. The difference of the criterion for design **2** and design **3** is less than one percent compared to the initial penalty value. Consequently, for future optimization runs reducing the number of generations could save computation time.

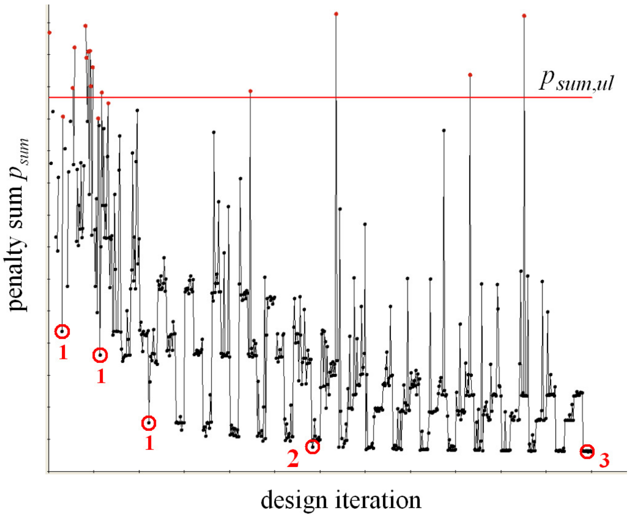


**Figure 12: Convergence history**

Figure 12 also reveals the typical behavior of a genetic optimization algorithm. In contrast to deterministic optimization algorithms, a genetic algorithm keeps diversity in its solution. The properties of the determined designs are allowed to vary at any time, which may lead to relative strong changes of the design criterion during almost the complete optimization. This diversity is one of the big advantages of applying genetic optimization algorithms as it allows to leave a local optimum and to determine a better solution during the search for the global optimum. It can be seen that already in the early stage of the optimization (between iteration one and one hundred) several solutions, **1** in Figure 12, have been generated having a considerably improved design criterion.

The eigenfrequencies of the solution, which were obtained by the optimizer, are shown in Figure 13. Compared to the initial design, Campbell diagram Figure 6, it can be seen that in general the eigenfrequencies have dropped and are free of resonance for all relevant excitation sources.

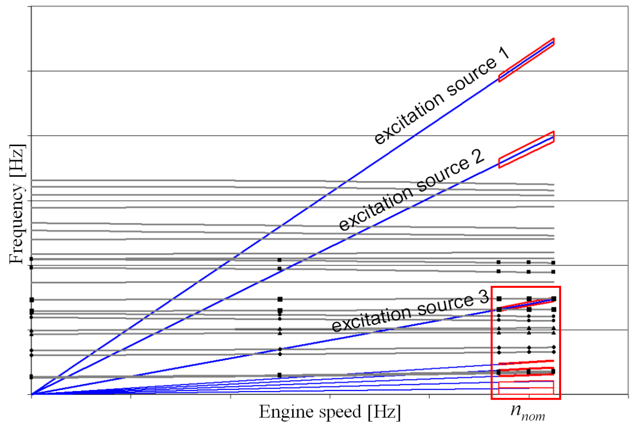


**Figure 13: Campbell diagram of optimized design**

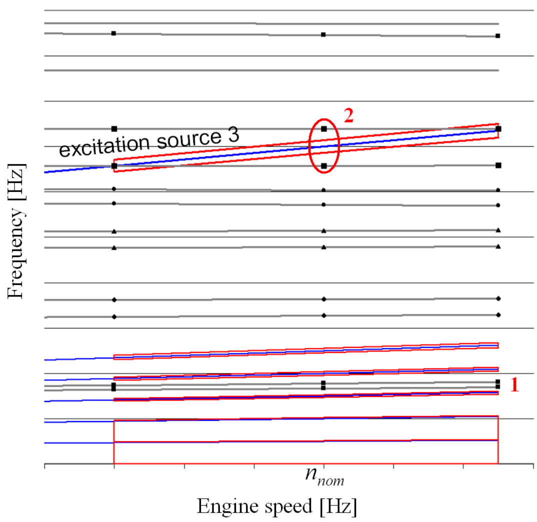


**Figure 14: Lower part of Campbell diagram of optimized design**

Considering the detailed view of the lower part of the optimized Campbell diagram, Figure 14, it can be determined that the first eigenmode pair is perfectly located between the excitation ranges of two lower engine orders, **1** in Figure 14. It is also observable, that one loose-tight mode pair has been shifted towards the forbidden area of excitation source 3, **2** in Figure 14. For nominal speed the calculated loose-tight eigenfrequencies are slightly above or below the prohibited frequency range of excitation 3. The reason, why the optimizer does not prevent resonance, which is caused by excitation 3, can be explained by the assignment of different excitation penalty values for different excitations, Table 2. Excitation caused by excitation source 3 receives the lowest penalty value (25) compared to excitation source 2 and excitations by lower engine orders (both 100) and excitation source 1 (50). The different penalty values let the optimizer keep the solution resonance free for the lower engine orders as well as for excitation sources 1 and 2 on the expense of violating the prohibited frequency range of excitation source 3.

The radial distribution of thickness and chord length of the new solution are shown in Figure 15 and Figure 16. Overall, it can be said that the optimized blade is characterized by a thinner airfoil decreasing the stiffness of the blade. The largest reduction in airfoil thickness was obtained at the tip section.

With respect to chord length the maximum change was obtained at the tip section as well. Increased chord values of the airfoil lead to a locally increased weight of the airfoil. At the lower 20 percent of the airfoil a local modification of the chord is obtained.

The radius of the transition fillet between airfoil and platform has been reduced. The locally increased mass of the airfoil in combination with the decreased stiffness causes the eigenfrequencies to drop considerably, which helped to achieve the optimization target.

In general, the optimized airfoil was characterized by a reduced mass of approximately five percent helping to reduce airfoil stresses in the transition from airfoil to platform.

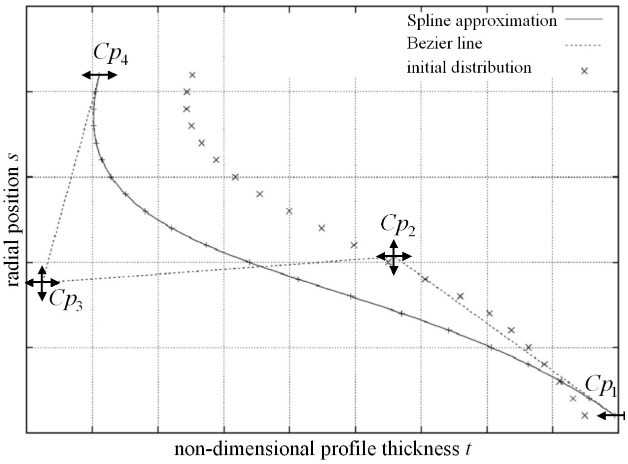


**Figure 15: Profile thickness development for optimized design**

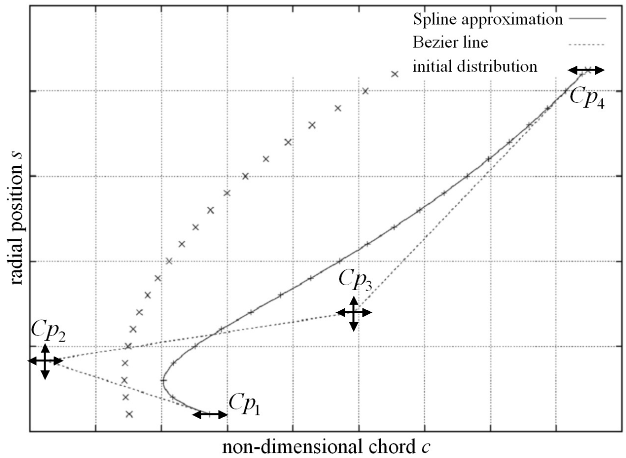


**Figure 16: Chord development for optimized design**

## CONCLUSIONS

The process for the mechanical analysis and frequency tuning of compressor blades was completely automated by applying Abaqus CAE and successfully implemented into the commercial optimization software iSight FD. The high level of automation, which was achieved in the FE model, set up and post-processing allowed a considerable reduction of the design time and enabled the consideration of more complex eigenmodes.

The determined design solution is resonance free for all relevant excitation sources. The strategy to apply penalty functions for frequency optimization has produced the expected results and an improved new design was obtained. The application of penalty functions, however, requires a good understanding of the critical eigenmodes and the excitation phenomena in the engine and needs care when being adjusted. The presented example has shown, that the optimizer will detect the weakness of the problem definition, i.e. in case a defined penalty value is not defined appropriately, eigenmodes may be pushed in resonance.

The optimization approach is to be understood as a feasibility study and is a first step towards applying numerical methods for solving complex blade dynamics problems. Prior to the application of the process for standard design tasks the sensitivity of the penalty functions needs to be looked at in more detail. Also, in order to reduce the computational effort the application of surrogate methods will be investigated in future work.

The results of this work are encouraging and future work is planned with the objective to introduce a multi-disciplinary optimization process by integrating the mechanical and aerodynamic design task into a single optimization process.

## REFERENCES


[1] Fedorov, I., Szwedowicz, J., Kappis, W. and Putchkov, I., 2010. "Reliable modeling of chord-wise blade modes in compressor design process". ASME Paper Number GT2010-22619, Glasgow, UK, June.

[2] Arkhipov, A. N., Pipopulo, A. V. and Putchkov, I. V., 2008. "Design tuning of high aspect ratio shrouded turbine blades". ASME Paper Number GT2008-50670, Berlin, Germany, June.

[3] Brophy, F., Mah, S. and Turcotte, J., 2010. "Preliminary multi-disciplinary optimization (PMOD) an example at engine level". NATO Lecture Series, RTO-EN-AVT-167 Strategies for Optimization and Automated Design of Gas Turbine Engines, Berlin, Germany, September.

[4] Walther, R., Frischbier, J. and Selmeier, R., 2001. „Aeromechanical Design of Advanced Engine Compressors". ISBAE Paper Number 1241, Bangalore India, September.

[5] Turner, M. G., Park, K., Siddappaji, K., Dey, S., Gutzwiller, D. P., Merchant, A. and Bruna, D., 2010. "Framework for multidisciplinary optimization of turbomachinery". ASME Paper Number GT2010-22228, Glasgow, UK, June.

[6] Demeulenaere, A., Ligout, A. and Hirsch, C., 2004. "Application of multipoint optimization to the design of turbomachinery blades". ASME Paper Number GT2004-53110, Vienna, Austria, June.

[7] Zheng, R., Xiang, J. and Sun, J., 2010. "Blade geometry optimization for axial flow compressor". ASME Paper Number GT2010-22229, Glasgow, UK, June.

[8] Ju, Y. and Zhang, C., 2010. "Multi-objective design method for tandem compressor cascade at design and off design conditions". ASME Paper Number GT2010-22655, Glasgow, UK, June.

[9] Karl, A., 2010. "Case study 3: Applications on component level: High pressure compressor and turbine discs, structural casings". NATO Lecture Series, RTO-EN-AVT-167 Strategies for Optimization and Automated Design of Gas Turbine Engines, Berlin, Germany, September.

[10] Karl, A., 2010. "Case study 4: Applications on subsystem level: Turbine system, secondary air system". NATO Lecture Series, RTO-EN-AVT-167 Strategies for Optimization and Automated Design of Gas Turbine Engines, Berlin, Germany, September.

[11] Pierret, S., Kato, H., Filomeno Coelho, R. and Merchant, A., 2006. "Aero-mechanical optimization method with direct CAD access – Application to counter rotating fan design". ASME Paper Number GT2006-90505, Barcelona, Spain, May.

[12] Siller, U. and Aulich, M., 2010. "Multidisciplinary 3D-optimization of a fan stage performance map with consideration of the static and dynamic rotor mechanics". ASME Paper Number GT2010-22792, Glasgow, UK, June.

[13] Pouzadoux, F., Reydellet, G., Taillefer, E. and Masmoudi, M., 2008. "Introduction of multi-disciplinary optimization in compressor blade design". 12th AIAA/ISSMO Multidisciplinary Analysis and Optimization Conference, Victoria, British Columbia, Canada, September.

[14] van den Braembussche, R. V., 2010. "Tuning of optimization strategies". NATO Lecture Series, RTO-EN-AVT-167 Strategies for Optimization and Automated Design of Gas Turbine Engines, Berlin, Germany, September.